

# Assessing the Quality of Wearable EEG Systems Using Functional Connectivity

Yacine Mahdid<sup>1</sup>, Uncheol Lee<sup>2</sup>, Stefanie Blain-Moraes<sup>1\*</sup>

<sup>1</sup>McGill University, Canada, <sup>2</sup>University of Michigan, United States

*Submitted to Journal:*  
Frontiers in Neuroscience

*Specialty Section:*  
Neuroprosthetics

*Article type:*  
Original Research Article

*Manuscript ID:*  
456373

*Received on:*  
25 Feb 2019

*Revised on:*  
31 Jan 2020

*Frontiers website link:*  
[www.frontiersin.org](http://www.frontiersin.org)

### *Conflict of interest statement*

The authors declare that the research was conducted in the absence of any commercial or financial relationships that could be construed as a potential conflict of interest

### *Author contribution statement*

SBM conceived of and designed the study. YM collected the data; YM and UL performed the analysis. SBM and YM wrote the first draft of the manuscript, which was edited and approved by all authors.

### *Keywords*

Electroencephalography - methods, Wearable Technology, functional connectivity, EEGapp, phase lag index (PLI)

### *Abstract*

Word count: 94

Assessing the data quality of wearable electroencephalographic (EEG) systems is critical to collecting reliable neurophysiological data in everyday environments. To date, measures of signal quality and spectral characteristics have been used to characterize wearable EEG systems. We demonstrate that functional connectivity metrics provide additional discriminatory information about EEG quality through an assessment of four wearable EEG systems (the Epoch+, OpenBCI, DSI-24 and Quick-30 Dry EEG) against a research-grade system (Electrical Geodesics Inc). Moreover, we provide a freely available Matlab toolbox containing these measures for the effective characterization of data quality from translational EEG devices.

### *Contribution to the field*

Collecting reliable neurophysiological data in everyday environments depends on high quality wearable electroencephalographic (EEG) systems. To date, wearable EEG systems have been assessed using measures of signal quality, spectral characteristics and event-related potentials. This technical note is the first to demonstrate that functional connectivity metrics provide additional discriminatory information about the quality of such systems, as demonstrated in an assessment of four commercially-available EEG headsets.

### *Funding statement*

This work was supported by the Natural Science and Engineering Research Council of Canada [grant number RGPIN-2016-03817].

### *Ethics statements*

(Authors are required to state the ethical considerations of their study in the manuscript, including for cases where the study was exempt from ethical approval procedures)

*Does the study presented in the manuscript involve human or animal subjects:* Yes

*Please provide the complete ethics statement for your manuscript. Note that the statement will be directly added to the manuscript file for peer-review, and should include the following information:*

- Full name of the ethics committee that approved the study
- Consent procedure used for human participants or for animal owners
- Any additional considerations of the study in cases where vulnerable populations were involved, for example minors, persons with disabilities or endangered animal species

*As per the Frontiers authors guidelines, you are required to use the following format for statements involving human subjects: This study was carried out in accordance with the recommendations of [name of guidelines], [name of committee]. The protocol was approved by the [name of committee]. All subjects gave written informed consent in accordance with the Declaration of Helsinki.*

*For statements involving animal subjects, please use:*

*This study was carried out in accordance with the recommendations of 'name of guidelines, name of committee'. The protocol was approved by the 'name of committee'.*

*If the study was exempt from one or more of the above requirements, please provide a statement with the reason for the exemption(s).*

*Ensure that your statement is phrased in a complete way, with clear and concise sentences.*

In this technical note, data from five different EEG headsets was collected from an author on the paper, exempting the study from the requirements of obtaining informed consent from the participants.

#### *Data availability statement*

Generated Statement: The datasets generated for this study are available on request to the corresponding author.

1 **Assessing the Quality of Wearable EEG**  
2 **Systems Using Functional Connectivity**

3 **Yacine Mahdid<sup>a</sup>, UnCheol Lee<sup>b</sup>, and Stefanie Blain-Moraes<sup>c</sup>**

4 <sup>a</sup>Integrated Program in Neuroscience, McGill University, 3801

5 University Street H3A 2B4, Montreal Quebec Canada

6 [yacine.mahdid@mail.mcgill.ca](mailto:yacine.mahdid@mail.mcgill.ca)

7 <sup>b</sup> Department of Anesthesiology, University of Michigan, 1500 East

8 Medical Center Drive, Ann Arbor, Michigan, USA

9 <sup>c</sup> School of Physical and Occupational Therapy, McGill University,

10 3654 Promenade Sir William Osler H3G 1Y5, Montreal, Quebec

11 Canada

12

13 Corresponding author: Stefanie Blain-Moraes

14 E-mail: [stefanie.blain-moraes@mcgill.ca](mailto:stefanie.blain-moraes@mcgill.ca)

15 Phone: 514-398-1325

16

17 Number of pages: 14

18 Number of figures: 7

19 Number of tables: 3

20    **Abstract**

21    Assessing the data quality of wearable electroencephalographic (EEG) systems is critical to  
22    collecting reliable neurophysiological data in everyday environments. To date, measures of  
23    signal quality and spectral characteristics have been used to characterize wearable EEG systems.  
24    We demonstrate that functional connectivity metrics provide additional discriminatory  
25    information about EEG quality through an assessment of four wearable EEG systems (the  
26    Epoc+, OpenBCI, DSI-24 and Quick-30 Dry EEG) against a research-grade system (Electrical  
27    Geodesics Inc). Moreover, we provide a freely available Matlab toolbox containing these  
28    measures for the effective characterization of data quality from translational EEG devices.

29    **Keywords:** electroencephalography; wearable technology; functional connectivity; EEGapp

---

30

31

32     **1. Introduction**

33       Effective translational research requires collecting neurophysiological data in non-laboratory  
34       settings. In response to the increasing demand for wearable electroencephalographic (EEG)  
35       systems, a range of ambulatory EEG technologies have been developed and used for clinical  
36       monitoring (e.g. epilepsy (Tatum IV et al 2001)); assistive technologies (e.g. (Wolpaw 2004));  
37       and monitoring the mental state of workers (Borghini et al 2014), drivers (Makeig and Inlow  
38       1993), and athletes (Thompson et al 2008). To date, the validation of wearable EEG systems has  
39       focused on comparisons to research-grade systems on the basis of 1) EEG signal quality; 2)  
40       spectral properties of continuous EEG recordings; and/or 3) the detection of event-related  
41       potentials (ERPs). EEG signal quality in wearable systems is typically assessed by the  
42       percentage of artifact-contaminated EEG, and the signal-to-noise ratio of the collected data  
43       (Barham et al 2017, Cruz-Garza et al 2017, Halford et al 2016, Mayaud et al 2013, Radüntz  
44       2018). Spectral properties are evaluated in relation to established phenomena, such as the Berger  
45       effect, and band power variation in relation to various tasks (Cruz-Garza et al 2017, Frey 2016,  
46       Grummett et al 2015, Halford et al 2016, Radüntz 2018). Finally, the ability to efficiently detect  
47       ERPs in various environments has often been used as a metric of the quality of a mobile EEG  
48       system (Barham et al 2017, Debener et al 2012, Frey 2016, Grummett et al 2015, Guger et al  
49       2012, Krigolson et al 2017, Mayaud et al 2013).

50           Functional connectivity has become a powerful tool for assessing neural phenomenon such  
51       as consciousness (Boveroux et al 2010, Jordan et al 2013, Lee et al 2013b, Ranft et al 2016), and  
52       has been used to characterize both neural dysfunction (Agosta et al 2012, Alexander-Bloch et al  
53       2010) as well as state transitions in the brain (Lee et al 2013a, Spoormaker et al 2010). Functional  
54       connectivity measures statistical dependences among remote neurophysiological events (Friston,

55 2011), and can be directed or undirected. Undirected functional connectivity can be calculated  
56 from phase coupling of band-limited oscillatory signals, or from coupled aperiodic fluctuations of  
57 signal envelopes (Engel et al., 2013). Common examples of techniques used to assess undirected  
58 functional connectivity (dependencies) include various measures of synchrony, correlation and  
59 coherence (Siegel et al., 2012). Directed functional connectivity metrics consider the temporal  
60 precedence of two signals. Prime examples of directed functional connectivity include partial  
61 directed coherence (Astolfi et al., 2006), directed transfer functions (Astolfi et al., 2005), Granger  
62 causality (Friston et al., 2013), symbolic transfer entropy (Staniek and Lehnertz, 2008), and  
63 directed phase lag index (Stam and van Straaten, 2012). While the application of functional  
64 connectivity metrics to EEG data has become increasingly popular, the quality of wearable EEG  
65 systems has never been evaluated according to these metrics. Of particular interest to the field of  
66 wearable EEG systems are the measures of phase lag index (PLI) and directed phase lag index  
67 (dPLI) due to their robustness against volume conduction and their low computational cost, which  
68 makes them ammenable to real-time calculation in a portal system. Moreover, PLI and dPLI have  
69 successfully been used to characterize brain network properties with significant clinical  
70 implications, including loss and recovery of consciousness (Blain-Moraes et al., 2014; Lee et al.,  
71 2013b, 2013a) and delirium (Dellen et al., 2014), and to identify network-level changes in  
72 conditions such as autism (Boersma et al., 2012), dementia (van Straaten et al., 2015) and fragile  
73 X syndrome (Molen et al., 2014).

74 In this technical note, we use signal quality, spectral measures and functional connectivity  
75 measures to evaluate and compare four wearable EEG systems against traditional research-grade  
76 equipment. Using a case example, we demonstrate that functional connectivity metrics provide  
77 complementary information to signal quality and spectral measures, and provide a freely available

78 Matlab toolbox containing these measures, which can be effectively used to assess the quality of  
79 wearable EEG systems.

80 **2. Methods**

81 *2.1 Electroencephalography Data Acquisition, Pre-processing and Analysis*

82  
83 EEG data were acquired from the headsets according to each of their respective best practices. **A.**  
84 **EGI 128-channel headset:** the electrode net was soaked in a solution of potassium chloride and  
85 baby shampoo for 10 minutes prior to application. The net was landmarked to Cz, and impedances  
86 were reduced to below 50 k $\Omega$  prior to initiating data recording. All channels were referenced to  
87 Cz, and data was collected at a sampling rate of 500 Hz. **B. Cognionics Quick-30:** This headset  
88 consisted of 30 dry electrodes that did not require any preparation prior to application. Electrode  
89 impedance was reduced to below 1 M $\Omega$  by removing the hair from under the electrodes and gentle  
90 abrasion of the scalp prior to data recording. All channels were reference to A2 and sampled at  
91 500 Hz. **C. Wearable Sensing DSI-24:** This headset consisted of 24 dry electrodes mounted on  
92 articulating bearings that maximized contact against the scalp. The electrode impedances were  
93 reduced to below 1 M $\Omega$  using a special tool that parted the hair around and below the electrodes.  
94 All channels were referenced to Pz and data was sampled at a frequency of 300 Hz. **D. EPOC+**  
95 **Emotiv:** This 14-channel headset consisted of electrodes with sponges that were soaked in  
96 Ag/AgCl saline solution for 10 minutes prior data collection. Impedance was reduced to below 20  
97 k $\Omega$  by parting the hair and moving the electrodes to make good contact with the scalp. All channels  
98 were referenced to P3/P4 and data were sampled at 256 Hz. **E. Open BCI:** This 8-channel system  
99 was composed of a Cyton 8-channel Biosensing Board, and a 3D printed headset which secured  
100 Dry Comb Electrodes. The system was fabricated and assembled according to instructions on the  
101 OpenBCI website (<http://docs.openbci.com>). It was not possible to measure electrode impedance,

102 thus, signal quality of each channel was assessed through visual inspection, and electrode positions  
103 were adjusted to maximize signal quality. Data were referenced to A2 and sampled at 250 Hz.

104 After data collection, the EEG was bandpass filtered using a finite impulse response filter  
105 between 0.1 and 50 Hz and re-reference to an average reference. All segments of data containing  
106 noise or non-physiological artifacts were identified by an investigator experienced in reading  
107 electroencephalograms and removed in EEGLab. Segments containing excessive sweat artefact  
108 (i.e. more than 2 standard deviations away from the mean) that persisted over 5 seconds were  
109 removed from the data. Segments containing high frequency electromyogram (EMG) artefacts  
110 were also removed from the data. Channels that did not record reliable EEG data (e.g. due to poor  
111 contact with the scalp) were identified through visual inspection of the waveforms and channel-  
112 specific spectrogram, and removed from the data. Electrooculogram (EOG) artefact was not  
113 removed from the EEG data from any headset; while techniques such as independent component  
114 analysis (ICA) would have effectively removed this artefact, they are more effective on headsets  
115 with higher numbers of channels, and this pre-processing step would have biased the subsequent  
116 analysis towards the high-density systems. The cleaned EEG was then analyzed using EEGapp, a  
117 freely available Matlab toolbox ([www.github.com/BIAPT/EEGapp](http://www.github.com/BIAPT/EEGapp)).

118 To compare the functional connectivity patterns between devices, the number of channels  
119 in the high-density system was decreased reduced to match the number of channels and channel  
120 locations of each of the wearable headsets. Each wearable headset was aligned to the gold standard  
121 system by matching all electrodes with 10-20 labels (e.g. Fz, C3, P4) to their corresponding  
122 counterparts. For all electrodes without a 10-20 label, the Euclidean distance to all nearest  
123 neighbours of the gold-standard headset was calculated using EGI's default 3D electrode location  
124 position file. Headsets were aligned using electrodes identified on the 10-20 system (e.g. Cz), and

125 ~~the Euclidian distances between all electrodes in the high-density headset and the wearable headset~~  
126 ~~were calculated.~~ Electrodes in the high-density system with the shortest distances to the electrodes  
127 in each of the wearable systems were selected as the candidate electrodes to generate comparative  
128 functional connectivity data.

129 *2.1.1 Spectral and Topographic Analysis.*

130 Spectrograms were computed using the multitaper method, using parameters listed in Table 2.  
131 Electroencephalographic data from all available channels were used in the analysis. Spectrograms  
132 from the wearable headsets were compared to the research-grade headset on the basis of the  
133 changes in delta and alpha power recorded during eyes-closed and eyes-opened conditions. Scalp  
134 power distributions at 10 Hz – the subject’s dominant alpha frequency - were also calculated across  
135 the average spectrogram using the topoplot function in EEGLab (Delorme and Makeig 2004).

136

137 *2.1.2 Functional Connectivity Analysis*

138 Functional connectivity between all combination of electrode pairs was assessed using phase  
139 lag index (PLI) and directed phase-lag index (dPLI). These metrics were chosen over other  
140 measures of functional connectivity such as coherence, as they are sensitive only to nonzero phase  
141 lead/lag relationships, and thus diminish the problem of volume conduction (Stam et al 2007). The  
142 instantaneous phase of each channel of the EEG was extracted using a Hilbert transform, and phase  
143 difference  $\Delta\varphi_t$  was calculated between channels, where  $\Delta\varphi_t = \varphi_{i,t} - \varphi_{j,t}$ ,  $t = 1, 2, \dots, n$ , where  
144  $n$  is the number of samples in one epoch and  $i$  and  $j$  included all channels in the EEG headset. PLI  
145 was then calculated as follows:

146 
$$PLI_{ij} = |\langle sign(\Delta\varphi_t) \rangle|$$

147 Here, the sign() function results in 1 if  $\Delta\varphi_t > 0$ , 0 if  $\Delta\varphi_t = 0$ , and -1 if  $\Delta\varphi_t < 0$ . Thus, a PLI  
148 value close to 1 indicates that the instantaneous phase of one signal is consistently ahead of  
149 another, and the phases are locked, whereas a PLI value close to 0 indicates no consistent phase  
150 lead or lag relationship between channels. The direction of the phase-lead/lag relationship between  
151 channels  $i$  and  $j$  were calculated using dPLI (Stam and van Straaten 2012).

152 
$$dPLI_{ij} = \langle H(\Delta\pi_t) \rangle$$

153 Here,  $H(x)$  represents the Heaviside step function, where  $H(x) = 1$  if  $x > 0$ ,  $H(x) = 0.5$  if  $x = 0$   
154 and  $H(x) = 0$  otherwise. Thus, if on average signal  $i$  leads signals  $j$ , dPLI will be between 0.5 and  
155 1, and if signal  $j$  leads signal  $i$ , dPLI will be between 0 and 0.5. If there is no phase-lead/phase-  
156 lag relationship between signals, dPLI = 0.5.

157 To quantify the effects of spurious phase relationships, surrogate datasets were calculated as  
158 follows. Hilbert transforms yielded the instantaneous phase of each combination of channel pairs  
159  $i$  and  $j$ . The phase time series of channel  $i$  was maintained, while in channel  $j$ , the phase time series  
160 from 0 to  $x$  was interchanged with the phase time series from  $x$  to  $n$ , where  $n$  is the number of  
161 samples in one epoch, and  $0 < x < n$ . Thus, existing phase relationships were eliminated while  
162 maintaining the spectral properties of each condition. The data were permuted according to the  
163 parameters listed in Table 3, and PLI and dPLI values were corrected by the characteristics of the  
164 surrogate dataset.

165 As the functional connectivity within both hemispheres of the brain were symmetric, PLI and  
166 dPLI results are only displayed for the left hemisphere, according to the schematic illustrated in  
167 Figure 1. While functional connectivity can be calculated for all frequencies, results were only  
168 displayed for the alpha bandwidth (8-13 Hz).

169 **2.1.3 Comparison of Wearable Systems to the Gold Standard**

170 Spectrogram were compared on the basis of whether the dominant powers in the wearable  
171 systems matched the frequency of the dominant powers in the gold standard. Topographic maps  
172 were compared based on the location of the dominant power in the different brain regions.

173

174 The PLI and dPLI matrices were compared against the gold standard using cosine similarity,  
175 defined as:

176

$$s = \frac{\mathbf{b}_i \cdot \mathbf{b}_j}{\|\mathbf{b}_i\| \|\mathbf{b}_j\|}$$

177 where  $\mathbf{b}_i$  and  $\mathbf{b}_j$  are the connectivity values for the wearable headset ( $i$ ) and the gold standard  
178 headset ( $j$ ) (Shin et al., 2013). Cosine similarity ranges from -1 to 1, where 1 indicates identical  
179 functional connectivity patterns between headsets, -1 indicates diametrically opposite functional  
180 connectivity patterns between headsets, and 0 indicates orthogonality or decorrelation.

181 **2.2 Case Example**

182 The added value of functional connectivity in assessing wearable EEG systems is demonstrated  
183 in a case example of a single participant (male, 24 years) using four wearable systems and one  
184 research-grade system (Table 1). In this study, we consider an EEG system wearable if it is mobile  
185 and wireless, enabling EEG to be performed outside of the laboratory (Barham et al., 2017); we  
186 compare it against a high-density, wired EEG system that is widely used in research studies. All  
187 systems were setup according to their respective best practices (e.g. acceptable levels of  
188 impedance). Continuous EEG was recorded in two 2-minute blocks: 1) eyes-closed rest; and 2)

189 eyes-open rest, and data from these single-trials were compared using three families of EEG  
190 analysis metrics described above.

191 To establish how representative these single-trial recordings were of performance across time,  
192 we collected 10 trials of eyes-closed rest and eyes-open rest from the same subject across five  
193 different days, at various times of day (i.e. morning, afternoon and evening) for two EEG systems.  
194 The three EEG analysis metrics were averaged across the ten trials, and the average spectrogram,  
195 topographic maps and functional connectivity matrices were compared to those computed for the  
196 single-trial recording.

197

### 198 **3. Results**

#### 199 *3.1 Signal Quality*

200 Two wearable EEG systems required that channels be removed from the subsequent data  
201 analysis due to the presence of non-physiological artifacts. Poor signal quality eliminated three  
202 channels in the Quick-30 system (Fp2, C2 and Cz), and two channels in the EPOC+ (AF4 and F2).  
203 The EEG channels used for subsequent analysis are displayed in Figure 2a.

#### 204 *3.2 Spectral and Topographic Analysis*

205 All systems detected the Berger effect - an increase in alpha power in the eyes-closed condition  
206 (Figure 2b). The posterior dominant rhythm was detected at 10 Hz in parietal and occipital regions  
207 in all EEG systems except for the EPOC+ (Figure 2c).

#### 208 *3.3 Functional Connectivity Analysis*

209 The gold standard of our functional connectivity analysis was generated from the research-  
210 grade EEG system. Posterior regions showed high functional connectivity during the eyes-closed  
211 condition, and central regions showed moderate functional connectivity during the eyes-open  
212 condition (Figure 3a, left column). A feedback lead/lag relationship dominated in posterior regions  
213 (e.g. from central to parietal, from central to occipital) in the eyes-closed condition, and was  
214 diffusely present in all regions in the eyes-open condition (Figure 3b, left column).

215 For ease of comparison to this gold standard, we present a subsampled version of the functional  
216 connectivity matrices adjacent to each wearable EEG system, with the electrodes from the gold  
217 standard selected to match with the location of each wearable system (Figure 3, column A).

218 The Quick-30 EEG system displayed significantly more frontoparietal and fronto-occipital  
219 functional connectivity than the gold standard in the eyes-closed condition, but had similar PLI  
220 patterns in the eyes-opened condition. Feedback connectivity was present in anterior regions (c.f.  
221 posterior regions in the gold-standard) during the eyes-closed condition, but similar to the gold-  
222 standard in eyes-open conditions (Figure 3, Quick-30 A versus B). Compared against the gold-  
223 standard, the PLI cosine similarity was 0.68 in the eyes-closed condition and 0.75 in the eyes-open  
224 condition; the dPLI cosine similarity was 0.84 in the eyes-closed condition and 0.91 in the eyes-  
225 open condition.

226 The DSI-24 EEG system presented higher functional connectivity across all electrode pairs in  
227 the eyes-closed condition, but similar patterns to the gold-standard in the eyes-open condition. It  
228 captured the posterior feedback lead-lag relationship, but also spurious centroparietal lead-lag  
229 relationships, in the eyes-closed condition. Lead/lag relationships were comparable to the gold-  
230 standard in the eyes-opened condition (Figure 3, DSI-24 A versus B). PLI cosine similarity was  
231 0.82 in the eyes-closed condition and 0.87 in the eyes-open condition; dPLI cosine similarity was

232 0.85 in the eyes-closed condition and 0.97 in the eyes-open condition.  
233 The EPOC+ EEG system presented spurious functional connectivity in the eyes-closed  
234 condition, and was unable to reproduce patterns of the eyes-open condition. Directed functional  
235 connectivity showed patterns opposite of those expected (e.g. feedforward lead-lag relationships)  
236 in the eyes-closed condition, and random lead/lag patterns in the eyes-opened condition (Figure 3,  
237 EPOC+ A versus B). Compared to the gold-standard, PLI cosine similarity was 0.85 in the eyes-  
238 closed condition and 0.79 in the eyes-open condition; dPLI cosine similarity was 0.92 in the eyes-  
239 closed condition and 0.75 in the eyes open-condition.

240 The OpenBCI Cyton Dry EEG system produced spurious functional connectivity between the  
241 parietal electrode and all other channels under both eyes-closed and open conditions. It did not  
242 capture the expected phase lead-lag relationship patterns under either condition (Figure 3,  
243 OpenBCI A versus B). PLI cosine similarity was 0.62 in the eyes-closed condition and 0.65 in the  
244 eyes-open condition; dPLI cosine similarity was 0.79 in the eyes-closed condition and 0.78 in the  
245 eyes-open condition.

246 Overall, the performance of the DSI-24 headset was most similar to the gold standard  
247 across both conditions and in both functional and directed functional connectivity measures  
248 (Figure 6).

#### 249 3.4 Comparison of Single Session to Averaged EEG characteristics

250 Spectrograms, topographic maps and functional connectivity matrices were compared for  
251 the EGI high-density system and the DSI-24 between a single session of recording data (e.g. one  
252 two-minute EEG epoch) and an average of ten 2-minute EEG epochs recorded at various times of  
253 the day during 5 different days. The single session data was similar to the averaged data across

254 both gold standard and wearable systems (Figure 7). Spectrogram power shows the greatest  
255 variability between single session and average data for both gold-standard and wearable systems,  
256 with greater alpha power in the single-trial data. Topographic maps show similar patterns of alpha  
257 power distribution across the brain, with alpha power dominant in posterior right brain regions.  
258 PLI functional connectivity patterns are strongly similar between single session and average data  
259 (gold standard cosine similarity = 0.97; wearable system cosine similarity = 0.991), as are dPLI  
260 functional connectivity patterns (gold standard cosine similarity = 0.995; wearable system cosine  
261 similarity = 0.999). This high degree of similarity demonstrates that the comparisons of headset  
262 performance based on single session data are representative of the average performance of the  
263 wearable systems.

264 **4. Discussion**

265 In this paper, we demonstrate that functional connectivity metrics can provide complementary  
266 information to signal quality and spectral measures in assessing the quality of wearable EEG  
267 systems. We compared four wearable EEG systems (the Quick-30, DSI-24, EPOC+ and  
268 OpenBCI) to a traditional research-grade EEG system from Electrical Geodesics Incorporated.  
269 Poor signal quality eliminated several channels from the Quick-30 and the EPOC+ from  
270 subsequent analysis. Spectral and topographic analysis resulted in similar performance across all  
271 wearable headsets, with the exception of the EPOC+. Here, the posterior dominant rhythm  
272 expected in the alpha bandwidth (Berger 1930) appears lateralized. However, signal quality and  
273 spectral analysis alone did not provide a granular distinction of the performance of the remaining  
274 three EEG systems. Assessing the systems with functional and directed functional connectivity  
275 provided additional information. The OpenBCI system was unable to produce the expected  
276 patterns of functional or directed functional connectivity. The Quick-30 and DSI-24 were able to

277 reproduce expected phase lead/lag relationships and patterns of dominant functional connectivity.  
278 While both systems were inferior to the gold standard (e.g. some spurious functional connectivity  
279 in the eyes-closed condition), this analysis demonstrated the integrity of the phase data recorded  
280 by each headset.

281 As measures of functional integration and connectivity become more dominant in the  
282 neuroscience literature (Friston 2011), there is increasing pressure to use these measures on EEG  
283 data recorded from translational, wearable headsets. Our analysis demonstrates the feasibility of  
284 applying functional connectivity analysis to EEG data collected from select wearable systems.  
285 Additionally, our results illustrate that the inclusion of functional connectivity metrics in the  
286 comparison of wearable EEG systems provides users with a more nuanced assessment of the  
287 quality of these systems.

288 Our demonstration of the added advantages of assessing translational EEG systems with  
289 functional connectivity measures need to be interpreted in light of several limitations. First, we  
290 evaluated the performance of the headsets on a single-subject basis, as opposed to a group-average.  
291 While this limits the generalizability of our results, we believe that the performance of a wearable  
292 EEG system on a subject-by-subject basis is strongly associated with its translational potential.  
293 The need for individualization in translational EEG applications has been established, as there is  
294 significant heterogeneity in EEG characteristics across the population (Cannon et al., 2014;  
295 Hammond, 2009; Loo and Makeig, 2012). Our case study enables us to compare the quality of  
296 the selected EEG heasets on a single-subject level, where idiosyncratic neural patterns – such as  
297 our participant's lateralized posterior dominant rhythm – are visible, as opposed to on a group  
298 level, where individual patterns are often averaged out. This within-subject comparison highlights  
299 the ability for wearable EEG systems to reproduce the subject-specific patterns that are visible in

300 the gold-standard EEG system, providing information that is more relevant to the translational  
301 potential of wearable headsets than a between-subject comparison. Thus, our method of  
302 comparing wearable EEG headsets on their ability to reproduce a single subject's idiosyncratic  
303 neural patterns through metrics such as cosine similarity was selected to address translational  
304 potential. Second, each headset had a different number and topographic distribution of electrodes.  
305 While we tried to account for this variability by downsampling the gold standard to the nearest-  
306 neighbour electrodes for comparison, this may bias the analyses for some headsets. For example,  
307 the Emotiv EPOC+ has a sparse distribution of electrodes in posterior brain regions, which will  
308 skew the alpha (10 Hz) topographic power map analysis towards frontal regions, in comparison to  
309 headsets with a more even electrode distribution. FinallyThird, we assessed the headsets only on  
310 the basis of one measure of functional connectivity (weighted phase lag index) and one measure  
311 of directed functional connectivity (directed phase lag index). While these metrics were chosen  
312 because of their robustness to volume conduction and their relatively low computational power  
313 (i.e. their translational potential), it is possible that other measures of functional connectivity (e.g.  
314 envelop-based connectivity metrics, information theory-based connectivity metrics) do not  
315 provide the same discriminatory power between headsets. Finally, all headsets were assessed on  
316 the basis of continuous rather than event-related EEG metrics. The ability to robustly detect ERPs  
317 in various environments has often been used as a marker of quality of mobile EEG headsets; the  
318 results presented in this paper provide a complementary assessment to this popular approach, and  
319 are particularly relevant for translational EEG applications focused on characterizing connectivity  
320 patterns in brain networks.

321 To accompany this article, we developed a freely available open-source Matlab toolbox for  
322 spectral, topographic and functional connectivity analysis ([www.github.com/BIAPT/EEGapp](http://www.github.com/BIAPT/EEGapp)).

323 Our toolbox enables non-experts to conduct these analysis on EEG collected from both wearable  
324 and research-grade systems, and automates many sections of the analysis (e.g. comparison of  
325 functional connectivity against surrogate data) that are required to accurately interpret the results.  
326 The open-source nature of our toolbox allows researchers to customize individual functions for  
327 their needs and to incorporate individual sections into larger analysis protocols.

328

329

330 **5. Conclusion**

331 Functional connectivity provides complementary information in the assessment of the quality  
332 of wearable EEG systems, and can be used to generate more nuanced distinctions between  
333 otherwise-comparable systems. The inclusion of this metric in wearable EEG system assessment  
334 is further warranted by the increasing interest in brain connectivity in the neuroscientific  
335 community. We provide an EEG analysis toolbox that allows researchers and non-experts to  
336 explore spectral and functional connectivity properties of EEG in hopes that the translational  
337 neuroscientific community will be able to benefit from and contribute to these tools.

338 **Acknowledgements**

339 The authors would like to thank Francesco Tordini from CIRMMT for lending us two of the  
340 EEG headsets, as well as Aaron Johnson for his help with the OpenBCI.

341 **Funding**

342 This work was supported by the Natural Science and Engineering Research Council of Canada  
343 [grant number RGPIN-2016-03817].

344

345 **References**

- 346 Agosta F, Canu E, Valsasina P, Riva N, Prelle A, Comi G and Filippi M 2012 Divergent brain  
347 network connectivity in amyotrophic lateral sclerosis *Neurobiol. Aging.* **34** 419-27
- 348 Alexander-Bloch A F, Gogtay N, Meunier D, Birn R, Clasen L, Lalonde F, Lenroot R, Giedd J  
349 and Bullmore E T 2010 Disrupted modularity and local connectivity of brain functional networks  
350 in childhood-onset schizophrenia *Front. Syst. Neurosci.* **4** 147
- 351 Barham M P, Clark G M, Hayden M J, Enticott P G, Conduit R and Lum J A G 2017 Acquiring  
352 research-grade ERPs on a shoestring budget: A comparison of a modified Emotiv and commercial  
353 SynAmps EEG system. *Psychophysiology* **54** 1393–404
- 354 Berger H 1930 Über das Elektrenkephalogramm des Menschen II *J Psychol Neurol* **40** 160–79
- 355 Borghini G, Astolfi L, Vecchiato G, Mattia D and Babiloni F 2014 Measuring neurophysiological  
356 signals in aircraft pilots and car drivers for the assessment of mental workload, fatigue and  
357 drowsiness *Neurosci. Biobehav. Rev.* **44** 58–75
- 358 Boveroux P, Vanhaudenhuyse A, Bruno M-A, Noirhomme Q, Lauwick S, Luxen A, Degueldre C,  
359 Plenevaux A, Schnakers C, Phillips C, Brichant J-F, Bonhomme V, Maquet P, Greicius M D,  
360 Laureys S and Boly M 2010 Breakdown of within- and between-network Resting State Functional  
361 Magnetic Resonance Imaging Connectivity during Propofol-induced Loss of Consciousness:  
362 *Anesthesiology* **113** 1038–53
- 363 Cruz-Garza J G, Brantley J A, Nakagome S, Kontson K, Megjhani M, Robleto D and Contreras-  
364 Vidal J L 2017 Deployment of Mobile EEG Technology in an Art Museum Setting: Evaluation of  
365 Signal Quality and Usability *Front. Hum. Neurosci.* **11** doi:10.3389/fnhum.2017.00527
- 366 Debener S, Minow F, Emkes R, Gandras K and de Vos M 2012 How about taking a low-cost,  
367 small, and wireless EEG for a walk?: EEG to go *Psychophysiology* **49** 1617–21
- 368 Delorme A and Makeig S 2004 EEGLAB: an open source toolbox for analysis of single-trial EEG  
369 dynamics including independent component analysis *J. Neurosci. Methods* **134** 9–21
- 370 Frey J 2016 Comparison of an open-hardware electroencephalography amplifier with medical  
371 grade device in brain-computer interface applications *ArXiv Prepr. ArXiv160602438*
- 372 Friston K J 2011 Functional and effective connectivity: A review *Brain Connect.* **1** 13–36
- 373 Grummert T S, Leibbrandt R E, Lewis T W, DeLosAngeles D, Powers D M W, Willoughby J O,  
374 Pope K J and Fitzgibbon S P 2015 Measurement of neural signals from inexpensive, wireless and  
375 dry EEG systems *Physiol. Meas.* **36** 1469–84

- 376 Guger C, Krausz G, Allison B Z and Edlinger G 2012 Comparison of Dry and Gel Based  
377 Electrodes for P300 Brain–Computer Interfaces *Front. Neurosci.* **6** doi: 10.3389/fnins.2012.00060
- 378 Halford J J, Schalkoff R J, Satterfield K E, Martz G U, Kutluay E, Waters C G and Dean B C 2016  
379 Comparison of a Novel Dry Electrode Headset to Standard Routine EEG in Veterans: *J. Clin.*  
380 *Neurophysiol.* **33** 530–7
- 381 Jordan D, Ilg R, Riedl V, Schorer A, Grimberg S, Neufang S, Omerovic A, Berger S, Untergerher  
382 G, Preibisch C, Schulz E, Schuster T, Schröter M, Spoormaker V, Zimmer C, Hemmer B,  
383 Wohlschläger A, Kochs E F and Schneider G 2013 Simultaneous Electroencephalographic and  
384 Functional Magnetic Resonance Imaging Indicate Impaired Cortical Top–Down Processing in  
385 Association with Anesthetic-induced Unconsciousness: *Anesthesiology* **119** 1031–42
- 386 Krigolson O E, Williams C C, Norton A, Hassall C D and Colino F L 2017 Choosing MUSE:  
387 Validation of a Low-Cost, Portable EEG System for ERP Research *Front. Neurosci.* **11** doi:  
388 10.3389/fnins.2017.00109
- 389 Lee H, Mashour G A, Noh G-J, Kim S and Lee U 2013a Reconfiguration of network hub structure  
390 after propofol-induced unconsciousness *Anesthesiology* **119** 1347–59
- 391 Lee U, Ku S, Noh G, Baek S, Choi B and Mashour G A 2013b Disruption of frontal–parietal  
392 communication by ketamine, propofol, and sevoflurane *J. Am. Soc. Anesthesiol.* **118** 1264–1275
- 393 Makeig S and Inlow M 1993 Lapse in alertness: coherence of fluctuations in performance and  
394 EEG spectrum *Electroencephalogr. Clin. Neurophysiol.* **86** 23–35
- 395
- 396 Mayaud L, Congedo M, Van Laghenhove A, Orlikowski D, Figère M, Azabou E and Cheliout-  
397 Heraut F 2013 A comparison of recording modalities of P300 event-related potentials (ERP) for  
398 brain-computer interface (BCI) paradigm *Neurophysiol. Clin. Neurophysiol.* **43** 217–27
- 399 Radüntz T 2018 Signal Quality Evaluation of Emerging EEG Devices *Front. Physiol.* **9** doi:  
400 10.3389/fphys.2018.00098
- 401 Ranft A, Golkowski D, Kiel T, Riedl V, Kohl P, Rohrer G, Pientka J, Berger S, Thul A, Maurer  
402 M, Preibisch C, Zimmer C, Mashour G A, Kochs E F, Jordan D and Ilg R 2016 Neural  
403 Correlates of Sevoflurane-induced Unconsciousness Identified by Simultaneous Functional  
404 Magnetic Resonance Imaging and Electroencephalography *Anesthesiology* **125** 861–72
- 405 Spoormaker V I, Schröter M S, Gleiser P M, Andrade K C, Dresler M, Wehrle R, Sämann P G  
406 and Czisch M 2010 Development of a Large-Scale Functional Brain Network during Human  
407 Non-Rapid Eye Movement Sleep *J. Neurosci.* **30** 11379–87

- 408 Stam C J, Nolte G and Daffertshofer A 2007 Phase lag index: assessment of functional  
409 connectivity from multi channel EEG and MEG with diminished bias from common sources  
410 *Hum. Brain Mapp.* **28** 1178–93
- 411 Stam C J and van Straaten E C W 2012 Go with the flow: use of a directed phase lag index  
412 (dPLI) to characterize patterns of phase relations in a large-scale model of brain dynamics  
413 *NeuroImage* **62** 1415–28
- 414 Tatum IV W O, Winters L, Gieron M, Passaro E A, Benbadis S, Ferreira J and Liporace J 2001  
415 Outpatient seizure identification: results of 502 patients using computer-assisted ambulatory  
416 EEG *J. Clin. Neurophysiol.* **18** 14–19
- 417 Thompson T, Steffert T, Ros T, Leach J and Gruzelier J 2008 EEG applications for sport and  
418 performance *Methods* **45** 279–88
- 419 Wolpaw J R 2004 Brain-computer interfaces (BCIs) for communication and control: a mini-  
420 review *Suppl.Clin.Neurophysiol.* **57** 607–13
- 421

422 **Tables****Table 1. EEG Acquisition Systems Specifications**

<b>Headset</b>	<b>Number of Channels</b>	<b>Type of system</b>
Geodesic Sensor Net (Electrical Geodsics Inc.)	129	Wet
Quick-30 (Cognionics)	30	Dry
DSI – 24 (Wearable Sensing)	24	Dry
EPOC + (EMOTIV)	14	Wet
Cyton Board (OpenBCI)	8	Dry

423

**Table 2. Spectrogram and Topographic Map Parameters**

<b>Parameters</b>	<b>Values</b>
Frequency pass	1.00 Hz to 30.00Hz
Temporal smoothing median filter	10
Time-bandwidth product	2
Number of tapers	3
Windows length	2 seconds
Step size	0.10
Topographic map frequency	10.00 Hz

424

**Table 3. Functional Connectivity Analysis Parameters**

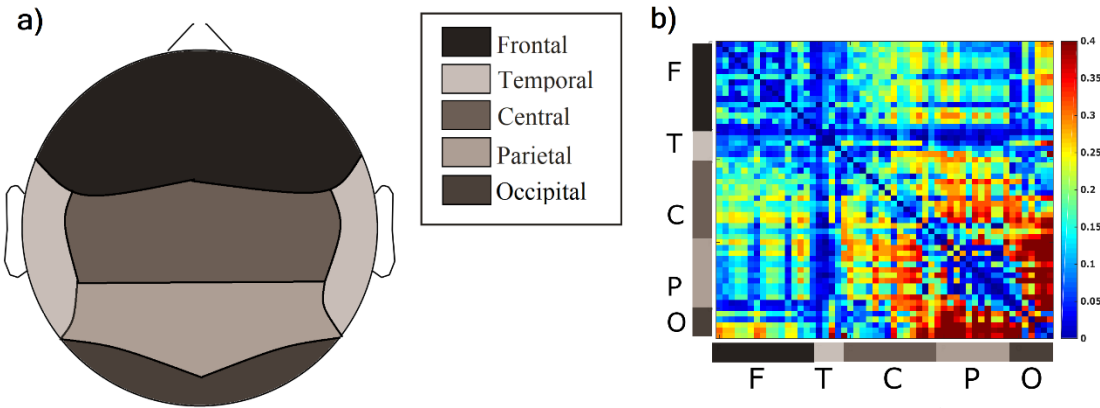
Parameters	Values
Length of analysis segments	10 seconds
Number of permutations	20
P value for surrogate data analysis	0.05
Bandpass filtering	8Hz to 13Hz

425

426

427

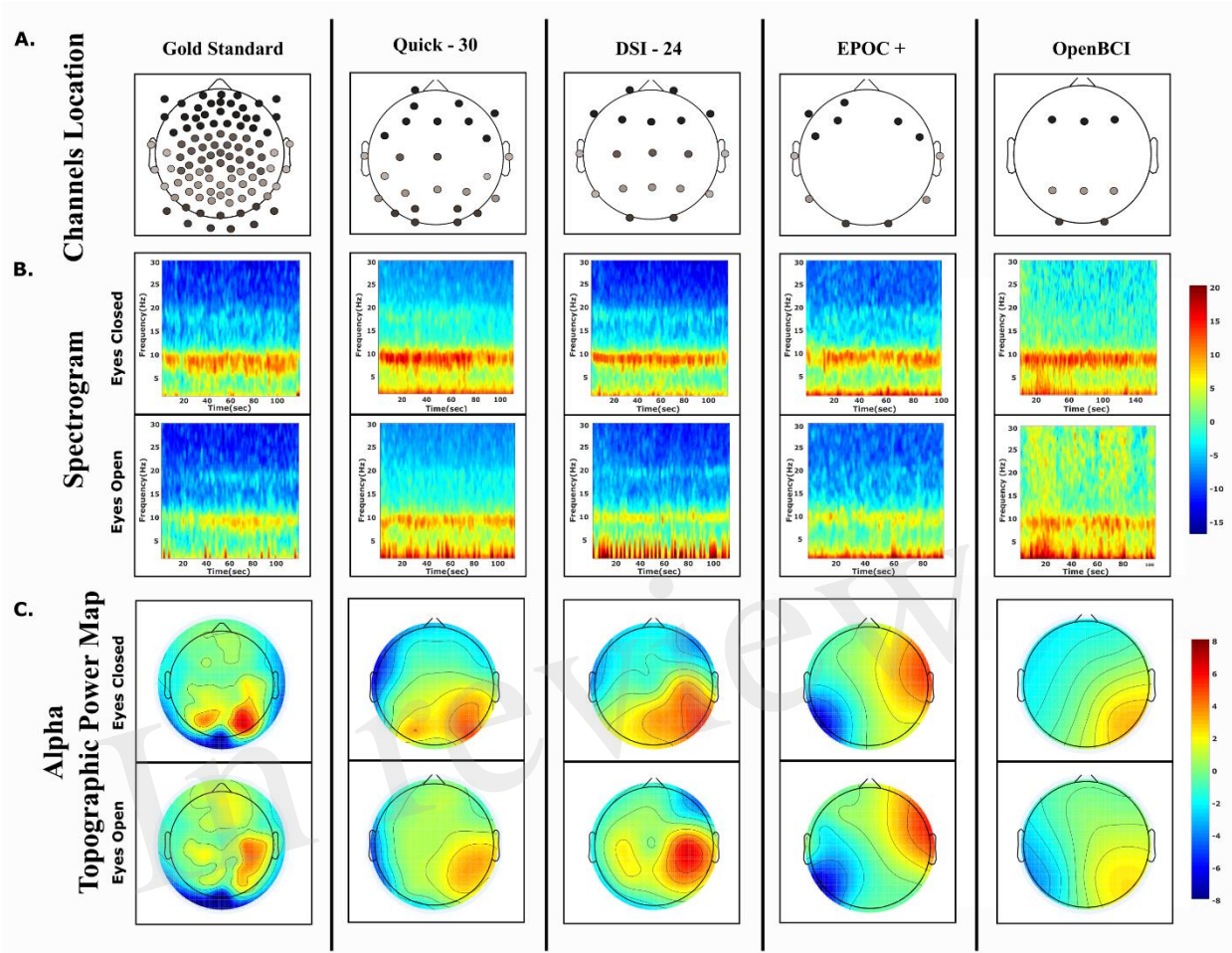
428 **Figures**



429

430 **Figure 1: Functional connectivity schematic.** a) Segmentation of the head for visualization of  
431 functional connectivity between all combinations of electrodes. b) Example left-hemisphere PLI  
432 matrix, generated using data from gold-standard system. The channels within each region are  
433 organized centrally to laterally, beginning at the anterior-most part of the region and following to  
434 the posterior-most part.

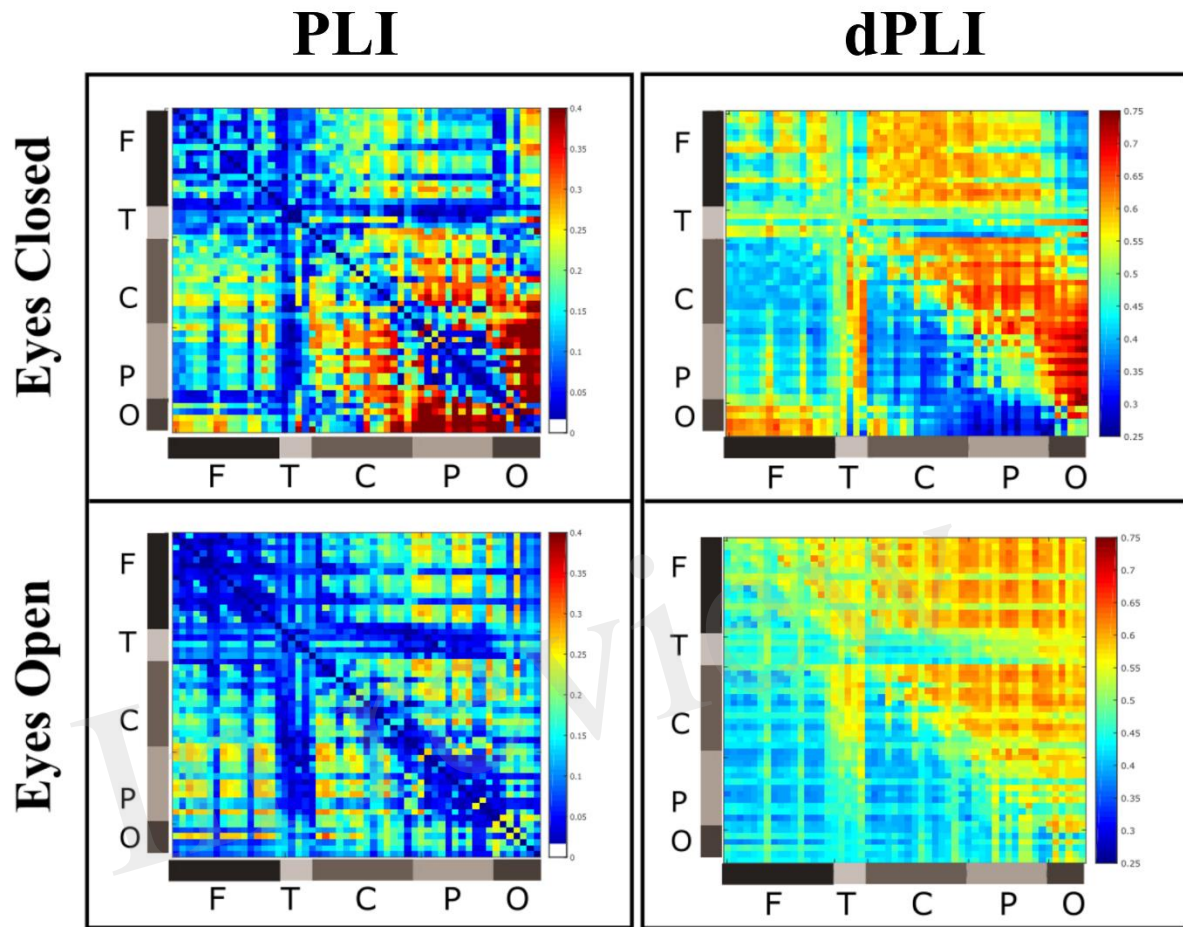
435



436

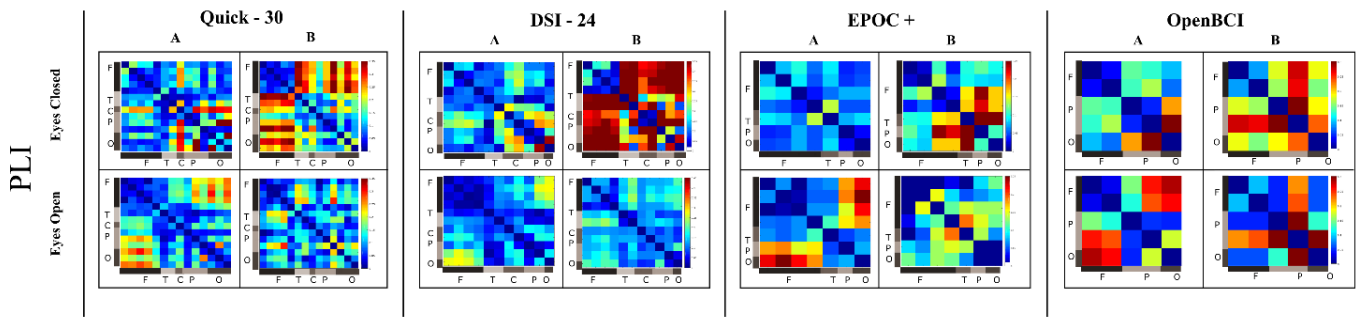
437 **Figure 2: Spectral and topographic analysis.** **Top row:** Location of the channels for the  
 438 Geodesic Sensor Net (i.e. gold standard), Quick-30, DSI-24, EPOC + and OpenBCI. **Middle row:**  
 439 Spectrogram across all channels for each EEG system for eyes-closed and eyes-open conditions.  
 440 **Bottom row:** Topographic power map at 10 Hz across the average spectrogram for each EEG  
 441 system under both conditions.

442

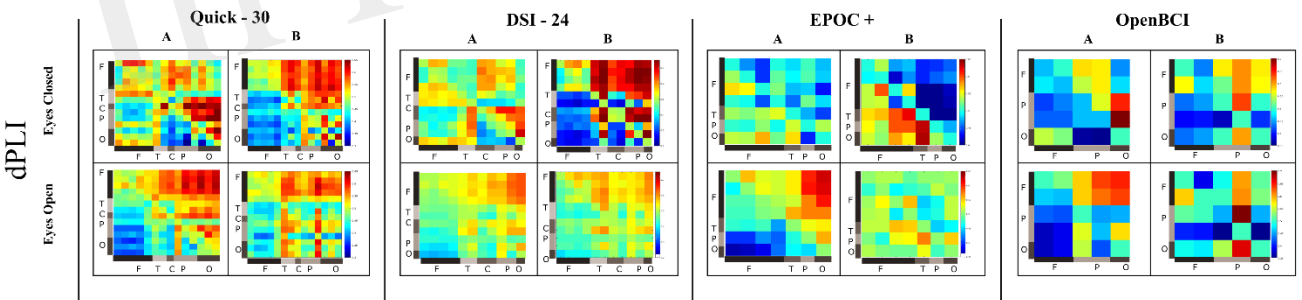


444 **Figure 3:** Functional connectivity (PLI) and directed functional connectivity (dPLI) matrices from  
 445 the research-grade EEG system during eyes closed and eyes opened conditions. PLI connectivity  
 446 is high in posterior regions during the eyes-closed condition; dPLI connectivity demonstrates  
 447 feedback lead/lag relationships across both conditions. F = frontal; T = temporal; C = central; P =  
 448 parietal; O = occipital.

449



451 **Figure 4:** Phase lag index (PLI) matrices across four wearable EEG systems. PLI matrices  
 452 generated from the corresponding nearest-neighbour electrodes from the research-grade EEG  
 453 system (column A) are compared against PLI matrices generated from the wearable headset  
 454 (column B) for eyes closed and eyes opened conditions. F = frontal; C = central; T = temporal;  
 455 P = parietal; O = occipital.

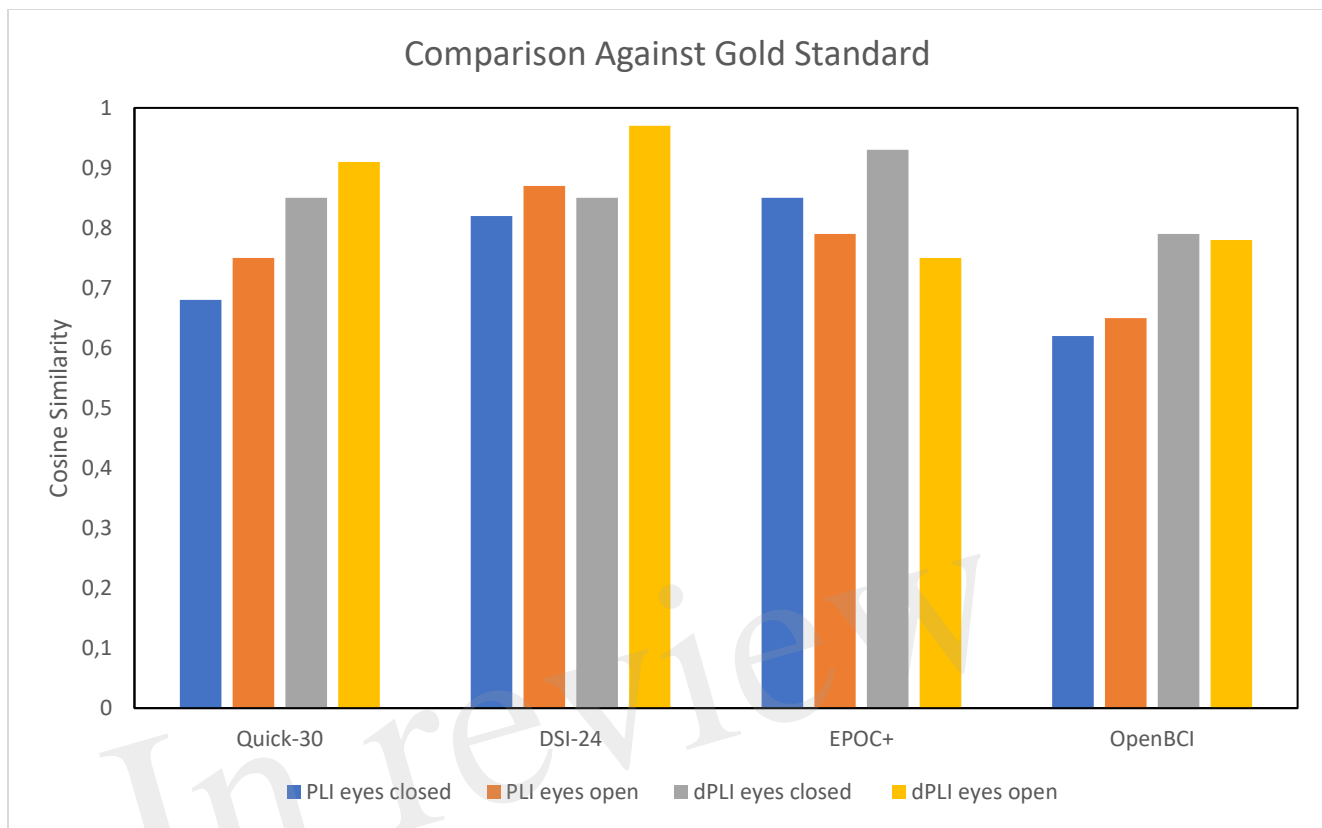


457 **Figure 5:** Directed phase lag index (dPLI) matrices across four wearable EEG systems. dPLI  
 458 matrices generated from the corresponding nearest-neighbour electrodes from the research-  
 459 grade EEG system (column A) are compared against dPLI matrices generated for the wearable  
 460 headset (column B) for eyes closed and eyes opened conditions. F = frontal; C = central; T =  
 461 temporal; P = parietal; O = occipital.

462

463

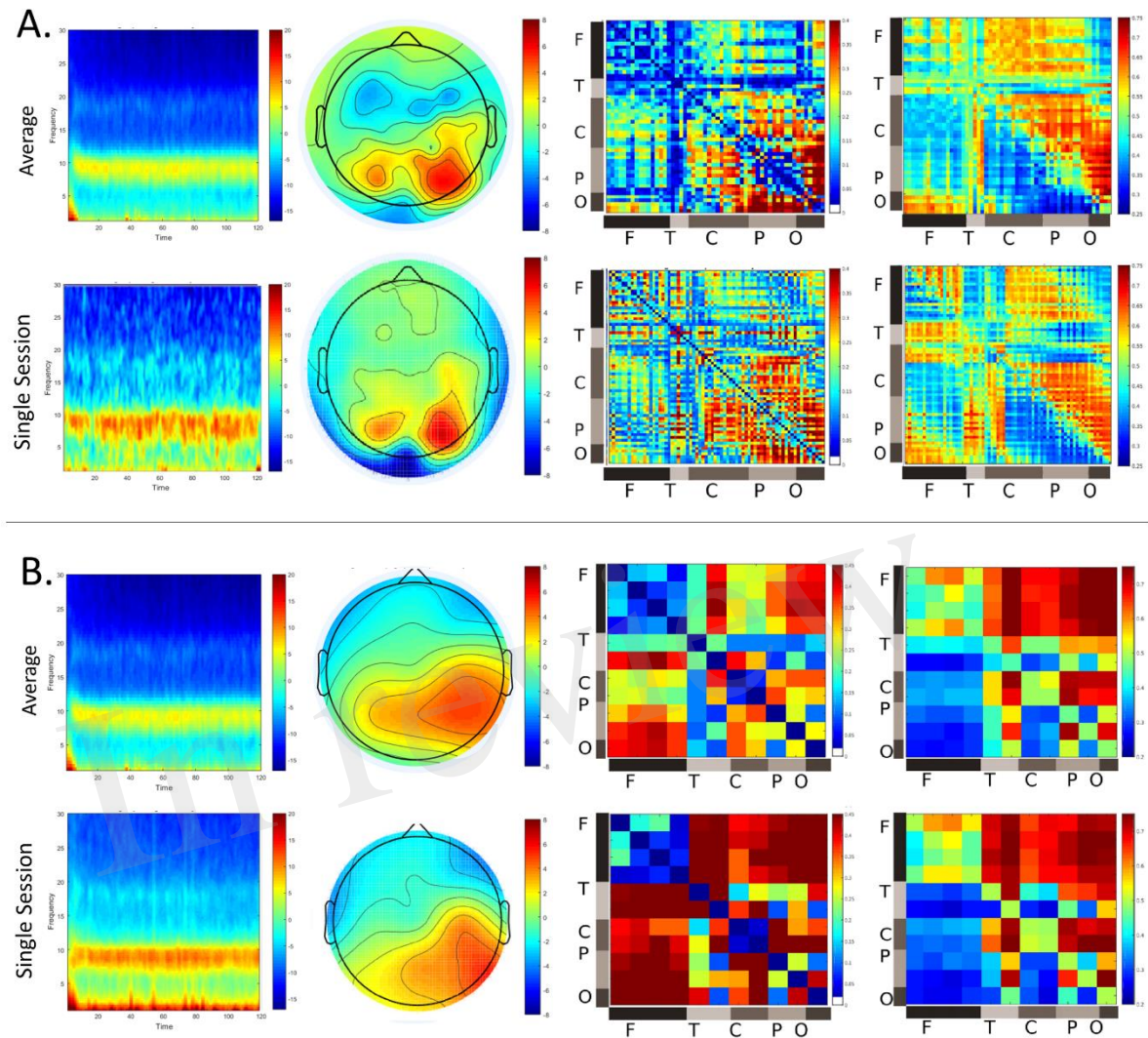
464



465

466 **Figure 6: Cosine similarity values of phase lag index (PLI) and directed phase lag index**  
 467 **(dPLI) calculated from each wearable EEG system compared to the gold standard.**

468



469

470 **Figure 7: Comparison of single session metrics to average metrics generated from 10**  
 471 **sessions recorded over multiple days for (A) research-grade (EGI) and (B) wearable (DSI-**  
 472 **24) EEG systems. Spectrograms, topographic maps, phase lag index and directed phase**  
 473 **lag index matrices show near identical (e.g. cosine similarity  $\geq 0.97$ ) patterns between single**  
 474 **session and averaged recordings.**

Figure 1.TIF



In review

Figure 2.TIF

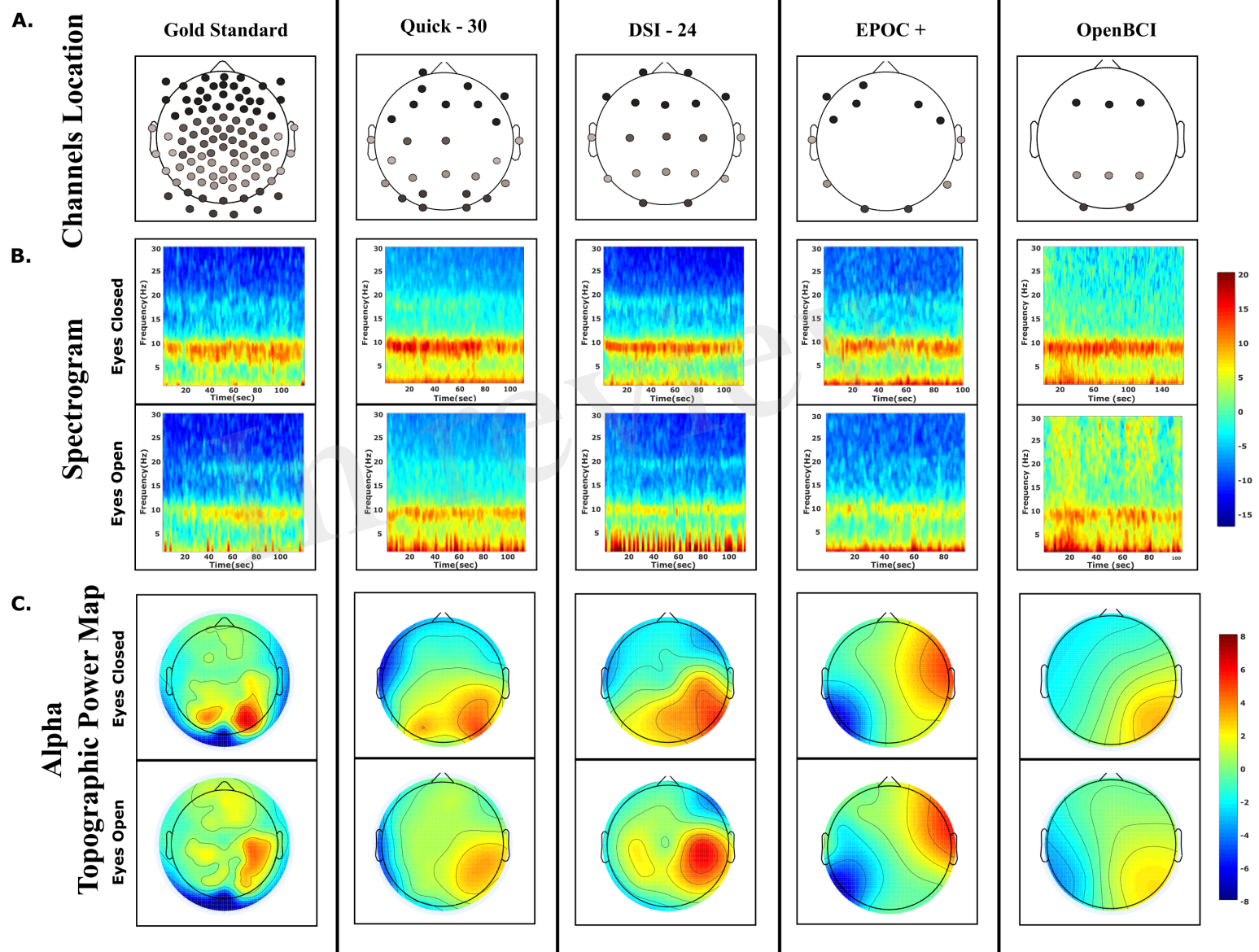


Figure 3.TIF

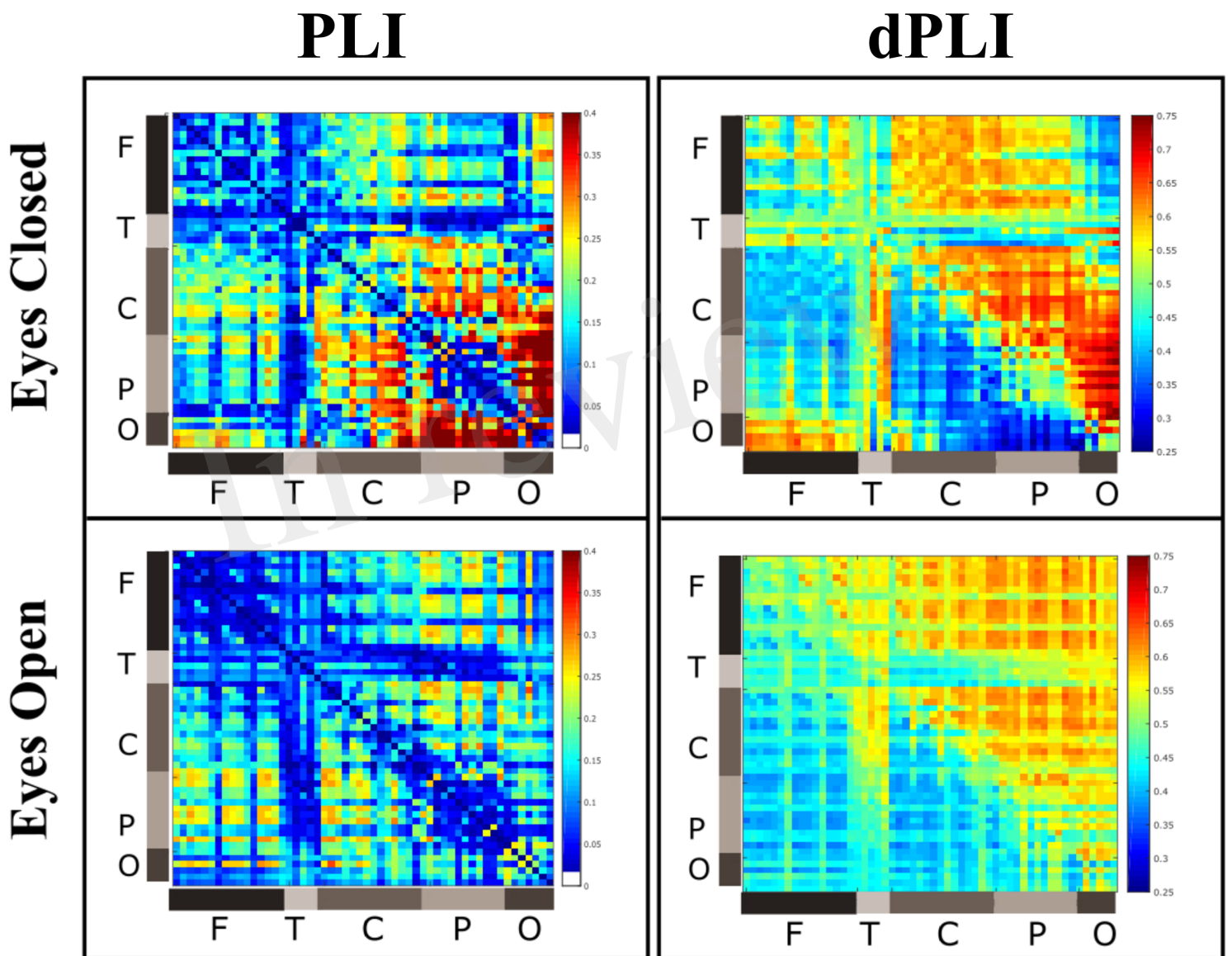


Figure 4.TIFF

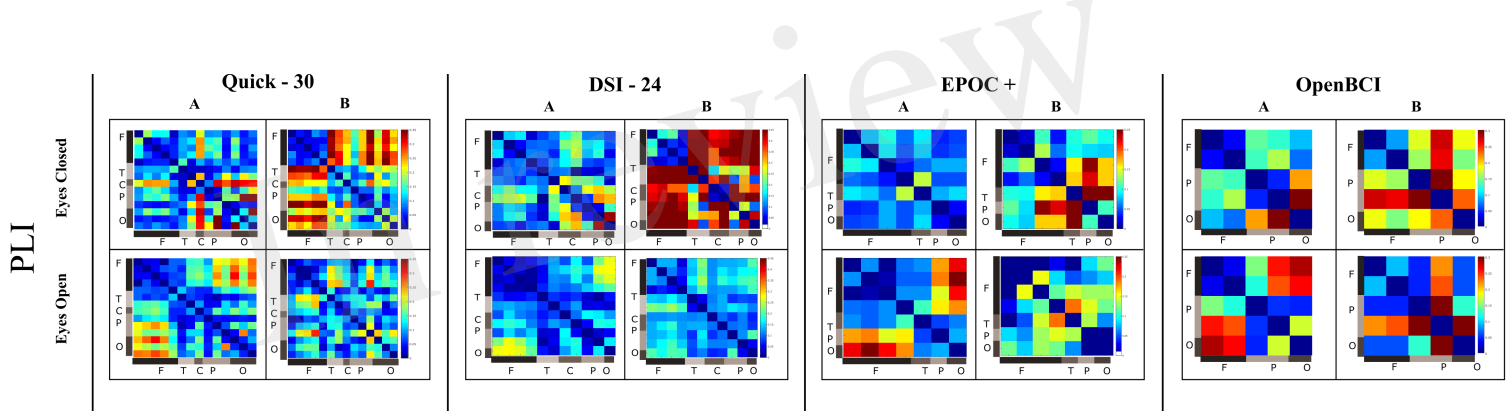


Figure 5.TIF

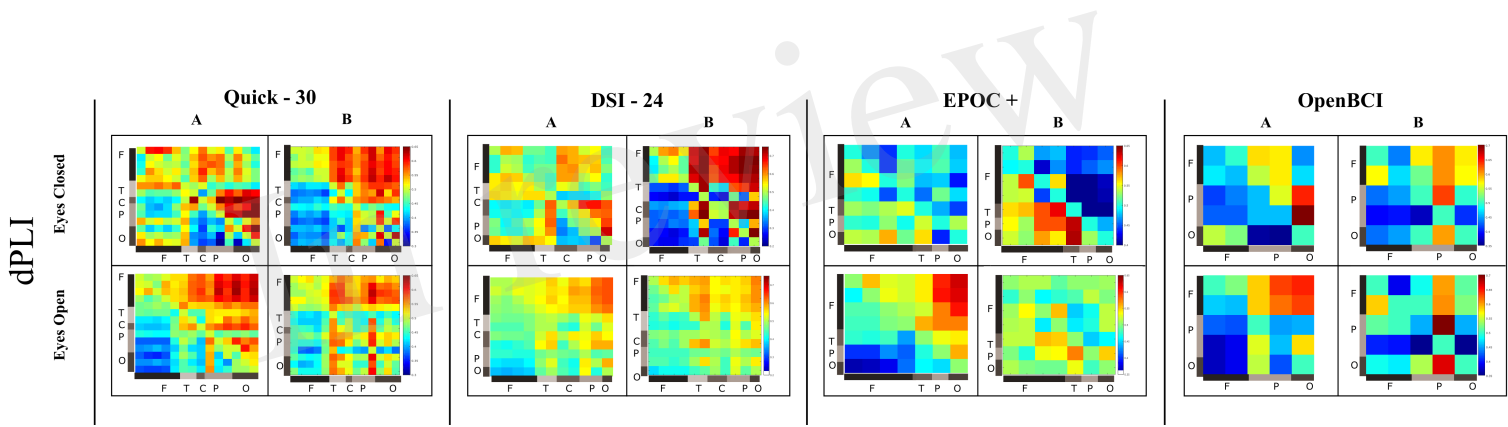


Figure 6.TIF

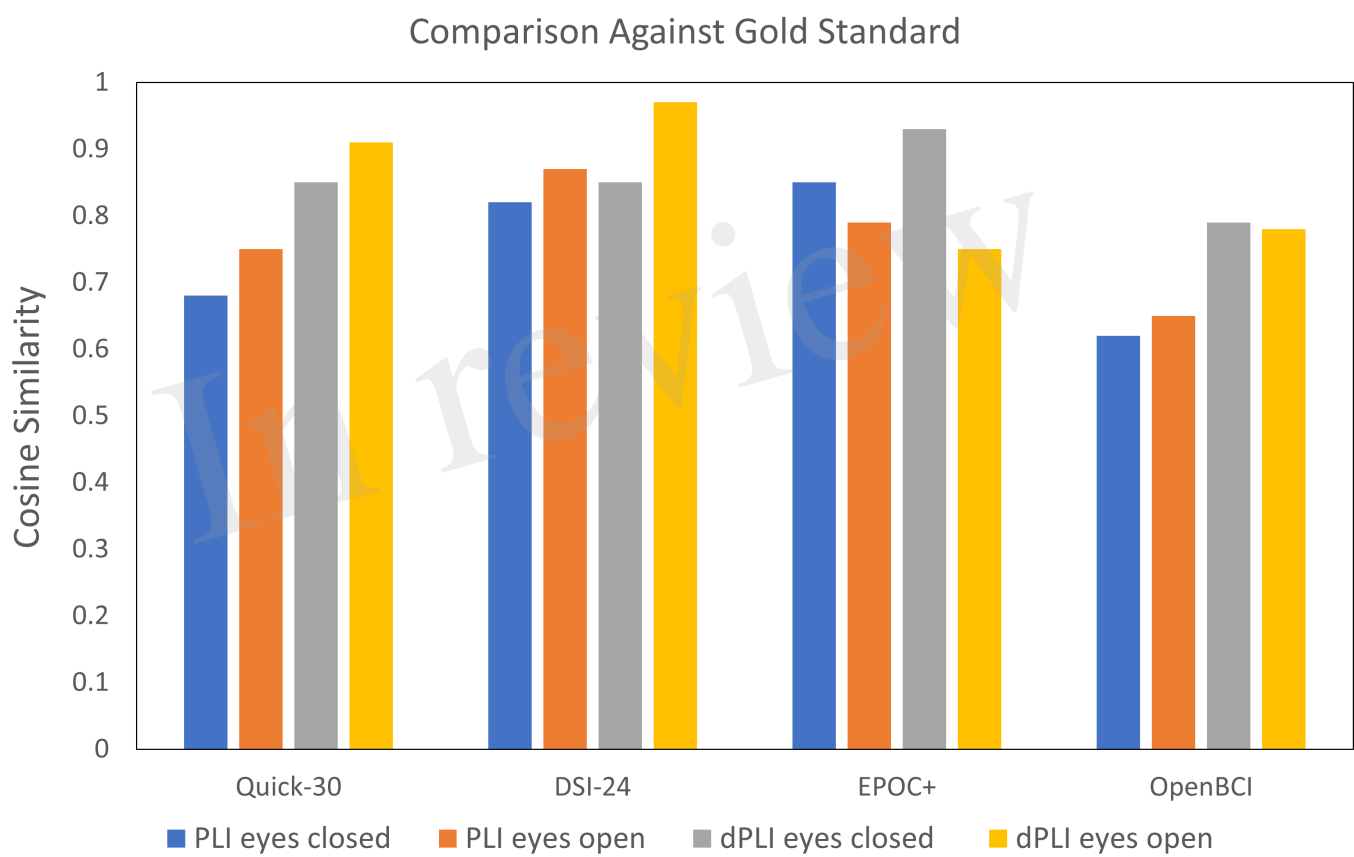


Figure 7.TIF

